Hydrogel–Silver Nanoparticle Composites: A New Generation of Antimicrobials

K. Varaprasad,[1] Y. Murali Mohan,[1]* S. Ravindra,[1] N. Narayana Reddy,[1] K. Vimala,[1] K. Monika,[2] B. Sreedhar,[3] K. Mohana Raju[1]

[1]*Synthetic Polymer Laboratory, Department of Polymer Science and Technology, Sri Krishnadevaraya University, Anantapur, Andhra Pradesh 515055, India*
[2]*Depatment of Microbiology, Sri Krishnadevaraya University, Anantapur, Andhra Pradesh 515055, India*
[3]*Inorganic and Physical Chemistry, Indian Institute of Chemical Technology, Hyderabad, Andhra Pradesh 500007, India*

Received 12 May 2009; accepted 3 August 2009
DOI 10.1002/app.31249
Published online 15 September 2009 in Wiley InterScience (www.interscience.wiley.com).

ABSTRACT: Design of consistant and eco-friendly methods for the synthesis of silver nanoparticles (AgNPs) is a significant forward direction in the field of application of antibacterial bionanotechnology. One among the available options is hydrogel templates, which are highly useful to achieve this goal. This investigation involves the development of poly(acrylamide)/poly(vinyl alcohol) hydrogel–silver nanocomposites (HSNCs) to achieve AgNPs of ~2–3 nm size in gel networks. The nanocomposite synthesis process is quite convenient, direct, and very fast, and the obtained hydrogel AgNP composites can be used for antibacterial and wound dressing applications. All the nanocomposite aqueous solutions have shown absorption peaks at 420 nm in UV–visible absorption spectrum corresponding to the Plasmon absorbance of AgNPs. X-ray diffraction spectrum of the HSNC exhibited 2θ values matching with silver nanocrystals. Transmission electron microscopy images of nanocomposites represent discrete AgNPs throughout the gel networks in the range of 2–3 nm. The developed nanocomposites were evaluated for antibacterial application on *E. coli*. © 2009 Wiley Periodicals, Inc. J Appl Polym Sci 115: 1199–1207, 2010

Key words: silver nanocomposites; semi-interpenetrated hydrogels; hydrogels; antibacterial activity; wound dressing; nanoreactors

INTRODUCTION

Monovalent silver such as silver nitrate and silver sulfadiazine are known for antibacterial activity because of oligodynamic effect.[1] The use of silver-based antimicrobial agents has emerged due to the fact that an increase of bacterial resistance to antibiotics caused by their wide spread use.[2] Although these topical agents exhibit superior bacterial inhibitions, there is a delay in the wound healing process. To solve this particular problem, silver is used in the form of colloidal suspension, i.e., silver nanoparticles (AgNPs).[3,4] An improved bactericidal activity is attributed to AgNPs because of their electronic effects that results a change in the local electronic structure of the surfaces of the nanosized particles, i.e., enhancement of the reactivity of AgNP surfaces. The AgNPs are capable of inactivating the vital enzymes and also help in prevention of the replication of DNA.[5] AgNPs were used to target the bacterial membrane to destabilize the plasma membrane potential that leads to the depletion of the levels of intracellular adenosine triphosphate, resulting in the death of bacterial cells. Many formulations based on AgNPs are effectively used for wound and burn dressings, surgical instruments, scaffolds, and skin donor.[6–11]

With an intention to provide an economically friendly products to the public, a number of synthetically varied methods were developed for AgNPs and AgNP composites by incorporating metal ions into the thin films of titania, sol–gels, polyelectrolyte multilayer films, porous polymers, AgNPs-doped biocompatible polymers, and viscous resins-loaded AgNPs.[12] Nanosilver-based wound dressings have received approval for clinical applications but dermal toxicity is reported.[13,14] Therefore, the combination of a gel system with AgNPs would be a better choice for the treatment of wounds in the form as such.[15] Three-dimensional

**Present address:* Cancer Biology Research Center, Sanford Research/USD, Sioux Falls, South Dakota 57105, USA.
Correspondence to: K. Mohana Raju (kmrmohan@yahoo.com).
Contract grant sponsors: Defence Research & Development Organization, The Ministry of Defence, Govt. of India, New Delhi.
Presented at MACRO-2009-Recent Advances in Polymeric Materials, Indian Institute of Technology (IIT), Chennai, March 9, 2009, Poster No.P31.

gel (nano-, micro, and hydrogel) networks are quite appropriate for the production of AgNPs than the conventional nonaqueous or polymers, biomacromolecules, dendrimers, liquid crystals, latex particles, etc.[16] The main reason for this is hydrogels can afford free space between the networks in the swollen stage serving for nucleation and growth of nanoparticles as nanoreactors or nanopots. This approach was established by Murali Mohan et al.[17] to obtain ~3 nm-sized AgNPs within the poly(*N*-isopropylacrylamide-*co*-sodium acrylate) hydrogel networks for antibacterial application purpose. Recent studies on AgNPs demonstrate that a biocompatible gel–silver nanocomposite helps for fast curing of wound burnings.[6–8]

As a part of our on-going laboratory program to develop biocompatible hydrogel–silver nanocomposite (HSNC) products[18] for efficient antibacterial materials, we have developed poly(acrylamide)/poly(vinyl alcohol) (PAM-PVA) HSNCs. In this investigation, we have taken PAM as a model gel, which is widely used for the number of applications, and PVA as an interpenetrating network polymer. PVA was taken because of its excellent wound dressing bioreactor property, controlled release, and blood adhesive properties in addition to reduction of silver salt and stabilization of AgNPs.[19]

EXPERIMENTAL

Materials

Poly(vinyl alcohol) (molecular weight, 125,000 and degree of acetylation, 19.5–22.7%) was purchased from S.D. Fine (Mumbai, India). Acrylamide (AM), 1,4-butanedioldiacrylate (BDDA), ammonium persulfate (APS) *N*,*N*,*N*′,*N*′-tetramethyl ethylenediamine (TMEDA), silver nitrate ($AgNO_3$), and sodium borohydride ($NaBH_4$) were obtained from Aldrich Chemical Company (Milwaukee, WI). Double distilled water was used throughout the investigation for the preparation of all solutions.

Preparation of hydrogels

Poly(acrylamide)/PVA hydrogels were prepared by an aqueous redox copolymerization using AM, a crosslinker (BDDA), and an APS/TMEDA initiating system in the presence of PVA at 25°C. In a typical polymerization reaction, 1 g of AM and 0.1 g of PVA were dissolved in 4 mL of distilled water by stirring for 5 min in 100 mL beaker. To this solution, 1 mL of BDDA (1 g/100 mL), 1 mL of APS (5 g/100 mL), and 1 mL of TMEDA (1 g/100 mL) solutions were sequentially added to the polymerization reaction mixture by stirring at 100 rpm on a magnetic stir plate. The gelation of the reaction was started instantaneously and the hard gel was formed within 30 min, but to get complete networks throughout the hydrogels, the reaction was continued for 8 h. The obtained gel sample was taken out of the beaker and washed with distilled water and placed in a 1-L beaker containing 500 mL distilled water (refilled fresh water for every 8 h for a week) to remove unreacted monomer/polymers from the gels. Finally, the gels were dried and cut into small pieces for further studies. The synthesized PAM-PVA hydrogels were transparent, suggesting homogeneous network structure. In a similar way, the gels were prepared by varying the reaction parameters such as concentration of PVA, BDDA, APS, and TMEDA. Table I describes the various components used to prepare PAM-PVA hydrogels.

Embedding the silver nanoparticles in hydrogels

In this process, dry hydrogels were immersed in large amount of distilled water for 2 days to swollen to full extent. Then, these hydrogels were transferred to a beaker containing 50 mL of 5 m*M* $AgNO_3$ aqueous solutions to permit equilibrating for 1 day. This step allows to load most of the silver ions by an exchange process from solution to hydrogel networks by anchoring through $-CONH_2$, and $-OH$ groups of hydrogel chains and the rest of metal ions were arrested in the free networks of hydrogels. Then, these silver ions-loaded gels were transferred into a beaker containing 50 mL of 10 m*M* $NaBH_4$ aqueous solution and allowed for 2 h to reduce the silver ions into AgNPs. The obtained AgNPs in the hydrogels are termed as HSNCs.

Characterization

Swelling studies

The swelling characteristic of the hydrogels provides the information about the hydrogel network integrity after loading silver salt and formation of embedded AgNPs inside the networks. To study this phenomenon, the same weights of dried hydrogels were equilibrated in distilled water at 25°C for 2 days. Swollen hydrogels were treated first with $AgNO_3$ and then with $NaBH_4$ solutions as mentioned in the sections "preparation of hydrogels" and "embedding the silver nanoparticles in hydrogels." The swelling ratio (Q) of the gels was calculated from the equation: $Q = W_e/W_d$, where W_e is the weight of the swollen hydrogel and W_d is the dry weight of the pure hydrogel.

FTIR spectrophotometer

FTIR spectrophotometer is used to identify the hydrogel formation, silver salt incorporation, and AgNPs formation in hydrogel networks. To record

TABLE I
Feed Composition of Poly(acrylamide)/Poly(vinyl alcohol)-Based Hydrogels Prepared by Using Free-Radical Solution Polymerization in the Presence of a Crosslinker (BDDA) and Redox-Initiating Pair (Ammonium Persulfate, APS and Tetramethyl Ethylenediamine, TMEDA)

	Concentration in the feed mixture of hydrogel networks				
Hydrogel code	AM (m*M*)	PVA (g)	BDDA (m*M*) $\times 10^{-4}$	APS (m*M*) $\times 10^{-3}$	TMEDA (m*M*) $\times 10^{-3}$
0P	14.08	0.00	5.044	2.191	1.721
1P	14.08	0.10	5.044	2.191	1.721
2P	14.08	0.15	5.044	2..191	1.721
3P	14.08	0.20	5.044	2.191	1.721
4PB	14.08	0.10	1.261	2.191	1.721
5PB	14.08	0.10	2.522	2.191	1.721
6PB	14.08	0.10	3.783	2.191	1.721
7PB	14.08	0.10	6.306	2.191	1.721
8PB	14.08	0.10	7.567	2.191	1.721
9PA	14.08	0.10	5.044	1.095	1.721
10PA	14.08	0.10	5.044	1.643	1.721
11PA	14.08	0.10	5.044	2.738	1.721
12PA	14.08	0.10	5.044	3.285	1.721
13PT	14.08	0.10	5.044	2.191	0.860
14PT	14.08	0.10	5.044	2.191	1.290
15PT	14.08	0.10	5.044	2.191	2.151
16PT	14.08	0.10	5.044	2.191	2.581

the FTIR spectra of hydrogel, Ag salts-loaded hydrogel, and AgNPs-embedded hydrogels, the samples were completely dried in an oven (Baheti Enterprises, Hyderabad, India) at 60°C for 6 h. These samples were read between 600 and 4000 cm^{-1} on a Bruker IFS 66V FTIR spectrometer (Ettlingen, Germany) using the KBr disk method.

UV–vis spectrophotometer

UV–vis absorption spectra of the samples were recorded on a Shimadzu 160A Model UV–vis spectrophotometer with a scan range of 200–600 nm. For this study, 100 mg of HSNC was dispersed in 10 mL of distilled water and allowed for 24 h to extract all AgNPs into aqueous phase and these solutions were recorded for absorption spectra.

X-ray diffraction

The X-ray diffraction (XRD) method was used to identify the formation of nanoparticles in the hydrogels. These measurements were carried out for dried and finely grounded samples on a Rikagu diffractometer (Cu radiation, $\lambda = 0.1546$ nm) running at 40 kV and 40 mA.

Transmission electron microcopy

Transmission electron microcopy (TEM) was used to determine the grain size of AgNPs embedded/formed inside the hydrogel networks. To image the silver nanocomposites on TEM, finely grounded HSNC samples were dispersed in 1 mL of distilled water and allowed to soak for 1 day to come out the AgNPs from the gel network into the aqueous phase. A total of 10–20 μL of this aqueous solution was dropped on a copper grid, removed the excess solution using filter paper, and dried at room temperature. The copper grid was inserted into Tecnai F12 transmission electron microscope (Philips Electron Optics, Holland) operating at an acceleration voltage of 15 kV.

Antibacterial activity

Method A. To examine the antibacterial effect of hydrogels, Ag^+ ion-loaded hydrogels, and HSNCs on a nutrient agar media, the agar medium was prepared by mixing 0.5 g of peptone, 3.0 g of beef extract, and 5.0 g of sodium chloride (NaCl) in 1000 mL distilled water, and the pH was adjusted to 7.0. Lastly, 15.0 g of agar was added to the solution. The agar medium was sterilized in a conical flask at a pressure of 15 lbs for 30 min. This agar was transferred into sterilized petri dishes in a laminar air flan. After solidification of the media, bacillus culture was streaked on the solid surface of the media. To this inoculated petri dish, one drop of gel solutions (20 mg/10 mL distilled water) was added using 50 μL tip and plates were incubated for 48 h at 37°C

Method B. The effect of bacterial growth of *E. coli* in mineral salts medium (MSM) was studied in the presence of AgNPs or HSNCs. This medium was

prepared by the following composition: NH_4NO_3 (1.5 g), KH_2PO_4 (2.5 g), K_2HPO_4 (0.5 g), NaCl (1.0 g), $MgSO_4$ (1.5 g), $MnSO_4$ (0.01 g), $FeSO_4$ (0.05 g), and $CaCl_2$ (0.05 g) were added to the 1000 mL of distilled water and the pH was adjusted to 7.0. Then, yeast extract (0.01%) was added for bacterial growth. After that the MSM medium was sterilized, 50 mL of solution was transferred into a sterilized 250-mL conical flask. Afterward, 100 μL *E. coli* bacterium was added into the media. Finally, 100 μL of AgNP solution (20 mg/10 mL distilled water) or its equivalent AgNPs suspension was added, and the optical density of the bacterial medium was measured using a UV–vis spectrophotometer at 600 nm.

RESULTS AND DISCUSSION

During the last few decades, a number of investigations were conducted to study the influence of AgNPs on various bacteria.[4] Because of their agglomerative nature in aqueous suspensions, the influence is not very much effective when compared with their highly dispersed stage and with a controlled release of AgNPs over a period of time. This property can be achieved when the AgNPs are embedded within the hydrogel networks.[17] Recent studies demonstrate that nanoparticles embedded into nano/micro/hydrogels or *in situ* generation of nanoparticles inside the gel networks leads to novel and advanced materials that can be applied directly to various diversified biomedical applications.[12] In our current strategy, the existence of PVA chains throughout the PAM hydrogel networks has not only regulated the gel networks but also influenced in controlling the silver salts, AgNPs formation, and embedding the nanoparticles into the gel networks. The main criteria in selecting PVA as an interpenetrating polymer in our hydrogels are its nontoxic, protecting, and steric stabilization properties that enhance the biomedical applications. Scheme 1 illustrates the preparation of PAM-PVA HSNCs.

Preparation of HSNCs

We have designed a universal HSNC system that can anchor an optimum number of AgNPs through PVA chains as well as PAM hydrogel networks, facilitating them a complete access to the surrounding aqueous media (swollen stage) to kill the bacteria with a balance attained between the water uptake capacity and gel integrity. The influence of PVA chains, the crosslink density, and the initiating pair in the composition of the resulted hydrogel templates on the AgNPs formation was investigated in detail.

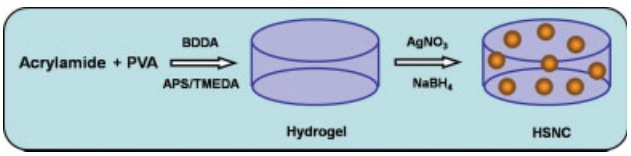

Scheme 1 Hydrogel–silver nanocomposite (HSNC) preparative schematic illustration in three steps. 1. Hydrogel synthesis from acrylamide and PVA in the presence of BDDA crosslinker and initiating pair. 2. Silver ions loading into hydrogel by placing hydrogel in silver nitrate ($AgNO_3$) solution for 24 h. 3. Silver ions into silver nanoparticles conversion: wiped off the gel containing silver ions then placed in sodium borohydride solution for 30 min. [Color figure can be viewed in the online issue, which is available at www.interscience.wiley.com.]

Hydrogel synthesis

It is well known that the synthesis of hydrogels by crosslinking polymerization involves a number of components including a monomer, polymer, crosslinker, and initiator/activator. The concentration of components not only maintains the reaction kinetics but also determines the characteristics of the resulting interpenetrated hydrogel networks especially the swelling capacity. PAM hydrogels (PAM) and PAM-PVA hydrogels (1P to 3P, 4PB to 8PB, 9PA to 12PA, and 13PT to 16PT) were prepared by redox-initiated free-radical crosslinking polymerization of aqueous mixtures of AM/PVA, BDDA crosslinker, and APS/TMEDA initiators for 8 h (Table I). Typically, most of the AM- or PNIPAM-based hydrogels and interpenetrated AM/PNIPAM hydrogels were formed rapidly by the free-radical crosslinking copolymerization within 30 min cure time, following the usual redox initiation mechanism. The redox initiation is further an efficient technique to produce gels with low soluble contents. A detailed representative schematic possible mechanism was demonstrated in our previous reports.[20,21]

The hydrogels with 0.10 g of PVA were selected for further modification of gels based on its higher swelling capacity in water [Fig. 1(a)]. The presence of polar moieties, i.e., PMA chains extend their hydrophilicity to the overall gel network in addition to the ion binding property. Further increase of PVA in the hydrogel networks does not contribute to increase in the swelling capacity that might be due to steric hindrance of PVA networks not allowing more water molecules in their networks. It was observed in our previous study of PAM/PVA that after an optimum concentration of PVA in the hydrogel network synthesis, the swelling capacity of the resulted hydrogel polymers either decreases or remains constant.[20,22] The crosslinker concentration is a major component that decides the swelling capacity of hydrogels. In our study, with the increase of BDDA concentration from 1.261–7.567 ×

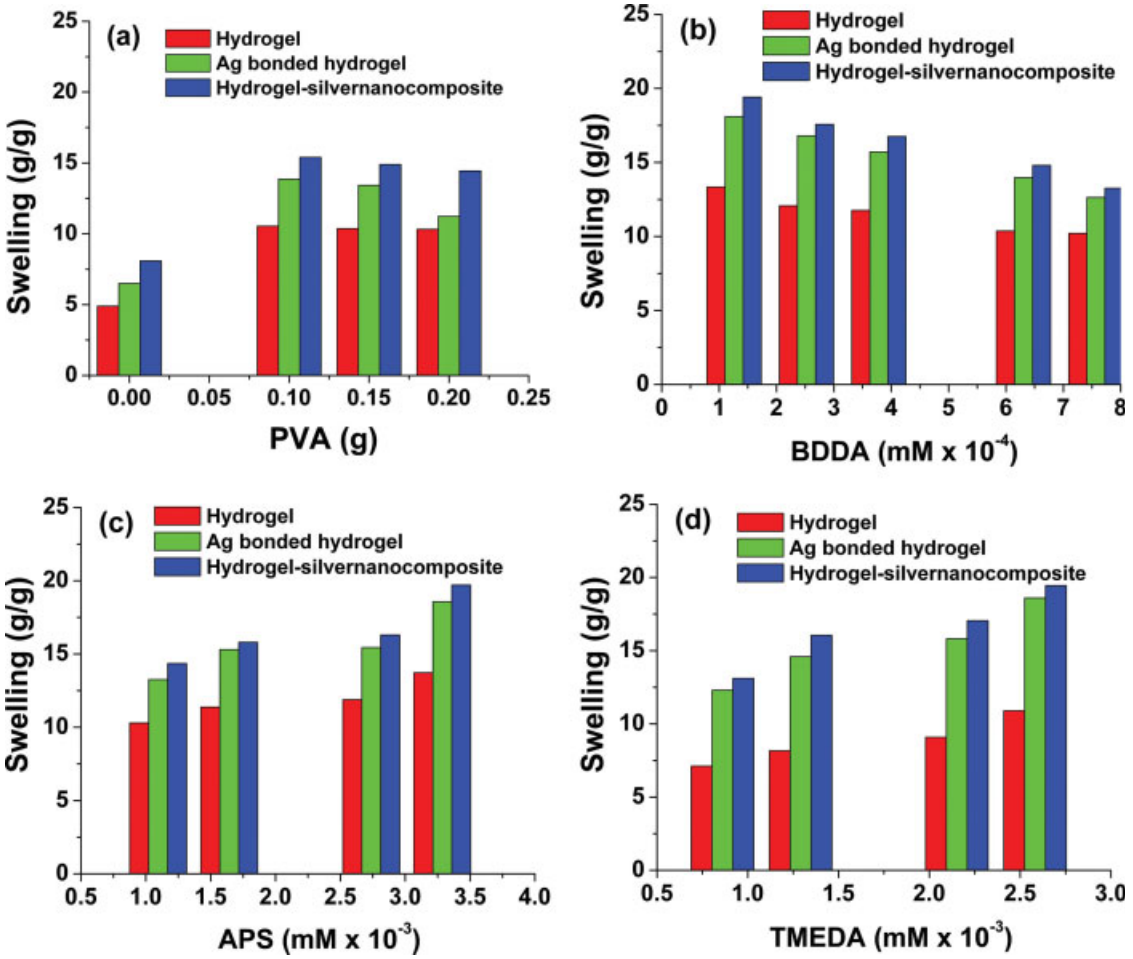

Figure 1 Swelling behavior of hydrogel, Ag^+-bonded hydrogel, and hydrogel–silver nanoparticles nanocomposites. (a) PVA variation, (b) crosslinker BDDA variation, (c) initiator APS variation, and (d) activator TMEDA variation in the hydrogel synthesis. [Color figure can be viewed in the online issue, which is available at www.interscience.wiley.com.]

10^{-4} M exhibits a slight decrease in the swelling capacity of the resulting hydrogels [Fig. 1(b)]. This is a common phenomenon with higher crosslinker content that makes the gel network denser, thereby restricting the penetration of the water molecules into the hydrogel networks. However, an increase in the concentration of APS or TMEDA increases from 1.095–3.285 $\times$ 10^{-4} M resulted in improved swelling characteristics of the hydrogel networks [Fig. 1(c,d)]. Overall, the swelling capacity of hydrogels at all PVA, BDDA, and APS concentrations has shown lower than MBA crosslinked hydrogels. The reason is that BDDA provides harder networks, which permit lower amounts of water than MBA crosslinked networks.[20,22]

Hydrogel–silver nanoparticle composites

The basic absorption and desorption of hydrogels are the key properties that can be used to load the metal ions and form the metal nanoparticles by reduction reaction. The hydrogel networks also control the particle size, shape, and its release from their networks, which are important for antibacterial activity or wound healing processes. The mechanism of AgNPs formation or embedded nanoparticles inside the hydrogel networks was similar to the procedure developed for PNIPAM-based hydrogels.[17] All the PAM-PVA hydrogel networks embed/anchor Ag nanoparticles effectively by the *in situ* process. Silver ions (Ag^+) were adsorbed from its silver nitrate solution into hydrogels by using the ion exchange ability of the amide groups of acrylamide units as well as the coordination capability of nitrogen atom in the AM of the hydrogel. The formed complexes with metal ion species inside the gel networks turn from transparent to brownish and enhance the hydrophilicity of networks that leads to an increased swelling capacity to the Ag^+-bonded hydrogels. Then, the Ag^+ ion-loaded hydrogels treated with $NaBH_4$ have turned into a dark brown color indicating the formation of AgNPs throughout the gel networks. During this step, the addition of many silver atoms to form the AgNPs with in the

TABLE II
Fourier Transform Infrared Spectral Data of the Hydrogel, Ag^+-Bonded Hydrogel, and Hydrogel–Silver Nanocomposite

Sample code	FTIR bands (cm^{-1})
6PB	3448.8, 2925.2, 2156.9, 1638.7, 1457.5, 1123.9, 617.9.
Ag^+-bonded 6PB	3424.9, 2930.3, 1654.6, 1458.1, 1381.5, 1119.4, 618.9.
Hydrogel–silver nanocomposite 6PB	3447.8, 2923.2, 2852.3, 1637.7, 1458.3, 1381.7, 669.2

For this hydrogel sample 6PB is used.

hydrogel networks expand the gel networks and promote higher water uptake capacity [Fig. 1(a–d)]. The increase in their swelling capacities is found to be directly proportional to their original hydrogel networks. The order of swelling capacity follows in this order, HSNC > Ag^+-bonded hydrogel > hydrogel (Fig. 1).

FTIR spectra

Table II illustrates the important peaks observed for hydrogel, Ag^+-loaded hydrogel, and hydrogel–AgNPs in FTIR spectra (Fig. 2). The main characteristic peaks were observed for 6PB hydrogel because of the presence hydrogen bonding between —NH_2 and —OH groups of PAM and PVA chains at (3448.8 cm^{-1}); amide I and II bonds of PAM (1654 and 1457.5 cm^{-1}); and C—O—H bending peaks of PVA (1123.9 $cm^{-1)}$. The silver-loaded hydrogel was also exhibited similar peaks but have much more broadened and also with a significant shift in the amide peak, i.e., 1654 cm^{-1} due to the complexation of silver ions with amide groups. When the silver ions are reduced to AgNPs, the FTIR peaks in all the positions were narrowed down, and the peak positions of hydrogen bonding in the samples and the

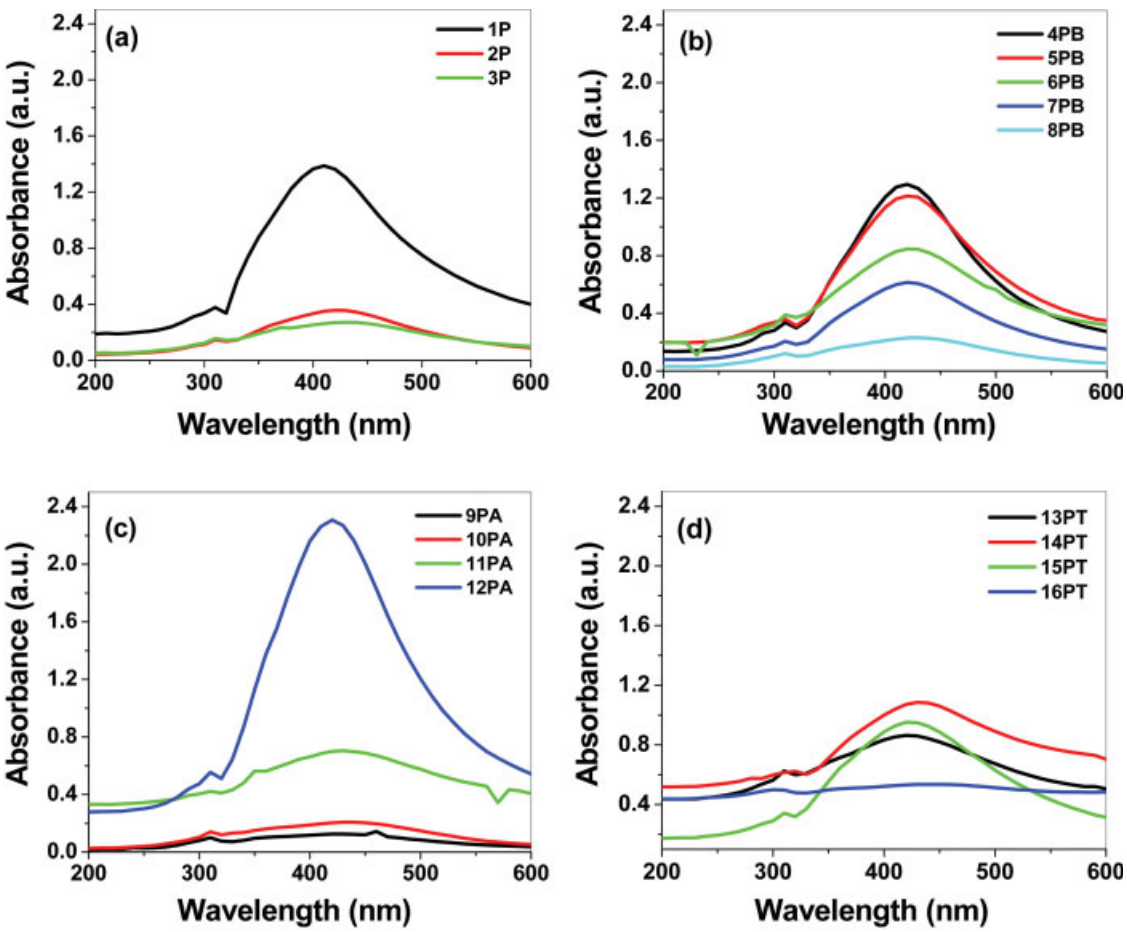

Figure 2 UV–vis spectra of the nanoparticles. HSNC prepared from hydrogels (a) 1P-3P, (b) 4PB-8PB, (c) 9PA-12PA, and (d) 13PT-16PT. [Color figure can be viewed in the online issue, which is available at www.interscience.wiley.com.]

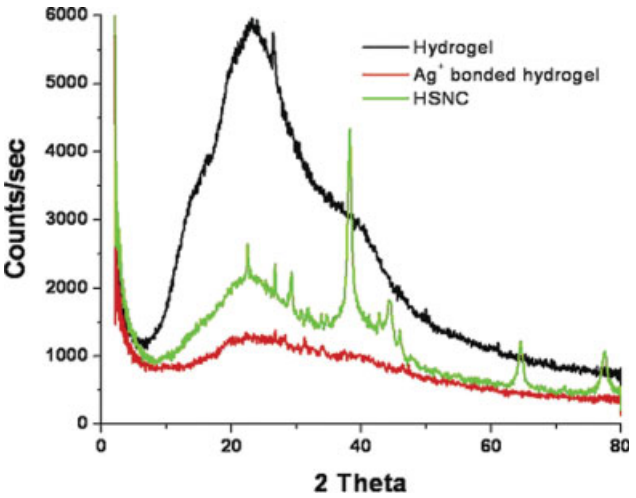

Figure 3 X-ray diffraction patterns of PVA-PAM hydrogel, Ag^+-bonded hydrogel, and hydrogel–silver nanocomposite. For this study, 4PB hydrogel code sample was used. [Color figure can be viewed in the online issue, which is available at www.interscience.wiley.com.]

amide peaks were relaxed to the same position as observed for 6PB hydrogel, thereby strongly demonstrating the formation of silver particles in the gels.

UV–vis spectra of HSNC

The formation of AgNPs can be analyzed easily by comparing the UV-spectra of solutions of pure silver nitrate and AgNPs. It is widely known that the peak can be observed at 298.3 nm for pure $AgNO_3$ solution corresponding to Ag^+ ions (data not shown), whereas for the solution of AgNPs the characteristic peak at 298.3 nm was decreased dramatically and a new peak was appeared at about 410 nm (Fig. 2), thus indicating the presence of Ag nanoparticles in the solution (10 mg in 1 mL of distilled water). With increase of PVA and BDDA concentrations in the composition of silver nanocomposites, UV maximum absorbency value has decreased [Fig. 2(a,b)]. The reason for this is that with the increase of PVA and BDDA crosslinks reduces the free volume of the hydrogel networks, and thereby less number of AgNPs is formed inside the gel networks. Figure 2(c) indicates that as the APS concentration increases in the preparation of silver nanocomposites the UV absorption also increases. As the initiator concentration increases more number of radicals is formed, there by resulting in less dense network polymer formation with increased free volume, allowing more silver particles into the gel. There was no consistency in the UV absorption peaks intensities with increase of TEMDA concentration in the HSNCs [Fig. 2(d)].

X-ray diffraction

The XRD pattern of hydrogel, Ag^+-bonded hydrogel, and silver nanocomposites was used to evaluate the nanoparticles formation in the gel networks (Fig. 3). Hydrogel and Ag^+-bonded hydrogels have not exhibited any sharp peaks in XRD. A broad peak at 25θ is due to the polymer networks. In the case of silver nanocomposite (4PB), sharp peaks are observed at 29.13, 38.14, 44.69, 64.38, and 77.51 θ, which can be corroborated to (111), (200), (220), (222), and (311) reflections, due to the formation of metallic AgNPs in the gel networks.

TEM analysis

The morphologies of the AgNPs were investigated by TEM images (Fig. 4). The TEM images clearly demonstrate that the nanoparticles formed inside the gel networks are spherical in shape. The obtained AgNPs in this investigation are 2–3 nm in size. The

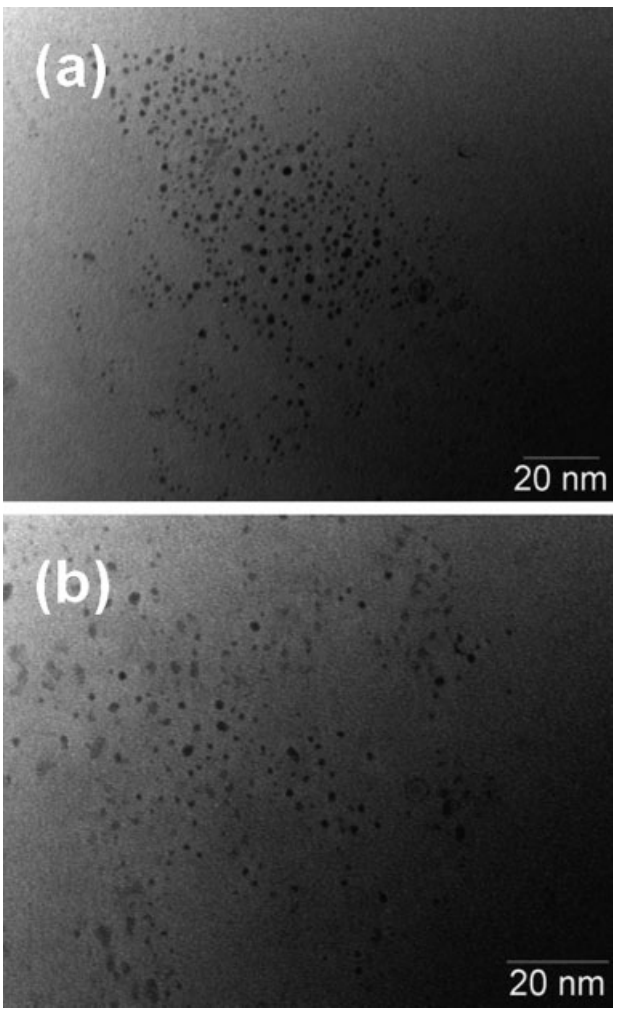

Figure 4 Transmission electron microscope images of hydrogel–silver nanocomposites prepared from (a) 4PB and (b) 7PB.

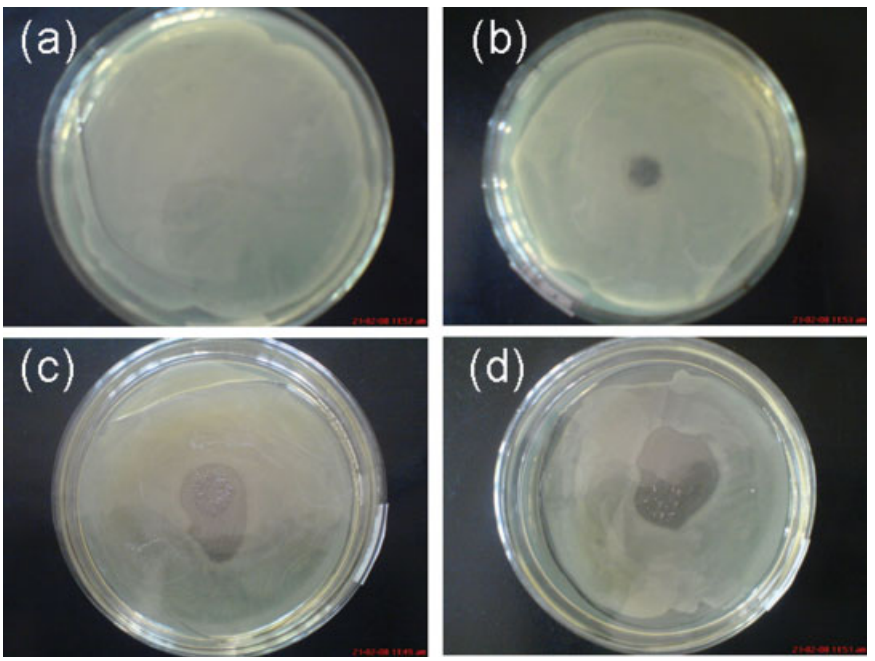

Figure 5 Antibacterial activity of (a) 7PB hydrogel, (b) 7PB Ag^{+}-bonded hydrogel, (c) silver nanoparticles, and (d) 7PB hydrogel–silver nanoparticle composite on *E. coli*. [Color figure can be viewed in the online issue, which is available at www.interscience.wiley.com.]

earlier reports confirmed that nanoparticles synthesized inside the networks of hydrogels vary and have larger size. The present achievement is due to change either in the monomer concentration or the BDDA concentration, which regulates the overall hydrogel mesh size which in turn judge the size of the particles. However, the current results suggest that the increase of crosslinker concentration (BDDA) only reduces the amount of particles in their networks but not the size of the particles. The reason in this case is due to high stabilization of the formed AgNPs by PVA networks. In all the previous cases, there was no efficient stabilizer in the hydrogel networks. Further, the obtained size of the AgNPs in the present networks is highly competitive (i.e., 2–3 nm in size) with respect to many of the previous reports of synthesis of AgNPs by various methods.

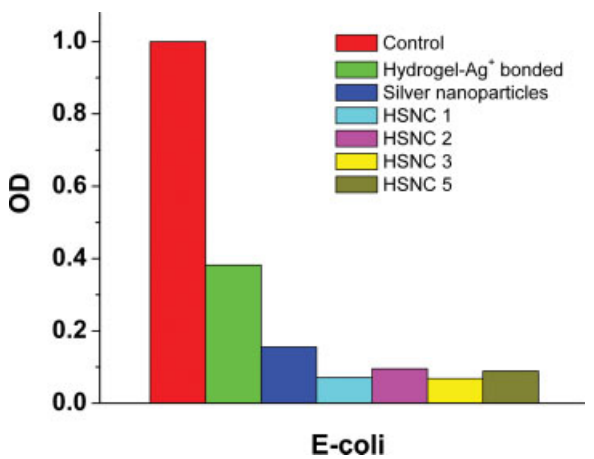

Figure 6 Antibacterial activity with silver nanoparticles and silver nanoparticles containing hydrogels (hydrogel–silver nanocomposites). [Color figure can be viewed in the online issue, which is available at www.interscience.wiley.com.]

Antibacterial activity

The antibacterial properties of the silver nanocomposites were tested with nutrient agar media. Figure 5 shows the typical antibacterial test results of hydrogel, Ag^{+}-bonded hydrogel, and silver nanocomposite. The AgNPs that having good dispersion capability throughout the hydrogel network were selected for the aforementioned studies. Figure 5(a) indicates that there is no effect of hydrogels on bacteria, whereas Figure 5(b) shows that the effect of silver ion-loaded hydrogels on the antibacterial activity is less when compared with AgNPs. The hydrogel–AgNPs showed the best antibacterial activity as shown in Figure 5(c). In addition, we have found that HSNCs exhibit higher activity on *E. coli* compared to AgNPs alone and Ag^{+}-bonded hydrogels (Fig. 6).

CONCLUSIONS

We have demonstrated a facile way to synthesize HSNCs that can be directly used for antibacterial and wound dressing applications. The size of the

silver particles is regulated to 2–3 nm by the PVA chains available throughout the hydrogel at all the crosslinker concentrations. Therefore, we propose that the PVA would be highly efficient stabilizer for the AgNPs in the hydrogels.

The authors thank B. Sreedhar for his valuable expertise on TEM analysis.

References

1. Masashi, C.; Tatsuo, Y.; Hideki, F.; Shinochi, N.; Zembee, N. J Antibact Antifung Agents 2004, 32, 115.
2. Ian, C. J Antimicrob Chemother 2007, 59, 587.
3. Petica, A.; Gavriliua, S.; Lungua, M.; Buruntea, N.; Panzaru, C. Mater Sci Eng B 2008, 152, 22.
4. Rai, M.; Yadava, A.; Gade, A. Biotech Adv 2009, 27, 76.
5. Yang, W.; Shen, C.; Ji, Q.; An, H.; Wang, J.; Liu, Q.; Zhang, Z. Nanotechnology 2009, 20, 085102.
6. Hwa Hong, K. Polym Eng Sci 2007, 47, 43.
7. Zhang, H.; Gu, C.-H.; Wu, H.; Fan, L.; Li, F.; Yang, F.; Yang, Q. BioFactors 2007, 30, 227.
8. Rujitanaroj, P.; Pimpha, N.; Supaphol, P. Polymer 2008, 49, 4723.
9. Sung Kim, J.; Kuk, E.; Nam Yu, K.; Kim, J.-H.; Jin Park, S.; Jang Lee, H.; Hyun Kim, S.; Kyung Park, Y.; Ho Park, Y.; Hwang, C.-Y.; Kim, Y.-K.; Lee, Y.-S.; Hong Jeong, D.; Cho, M.-H. Nanomed Nanotechnol Biol Med 2007, 3, 95.
10. Erdogan, B.; Rotello, V. M. Chem—Eur J 2004, 10, 5570.
11. Magdassi, S.; Bassa, A.; Vinetsky, Y.; Kamyshny, A. Chem Mater 2003, 15, 2208.
12. Thomas, V.; Namdeo, M.; Murali Mohan, Y.; Bajpai, S. K.; Bajpai, M. J Macromol Sci A 2008, 45, 107.
13. Chen, X.; Schluesener, H. J. Toxicol Lett 2008, 176, 1.
14. http://www.silvermedicine.org/medical-products-silver.html.
15. Murali Mohan, Y.; Premkumar, T.; Lee, K.; Geckeler, K. E. Macromol Rapid Commun 2006, 27, 1346.
16. Bajpai, S. K.; Murali Mohan, Y.; Bajpai, M.; Tankhiwale, R.; Thomas, V. J Nanosci Nanotechnol 2007, 7, 2994.
17. Murali Mohan, Y.; Lee, K.; Premkumar, T.; Geckeler, K. E. Polymer 2007, 48, 158.
18. Murthy, P. S. K.; Murali Mohan, Y.; Varaprasad, K.; Sreedhar, B.; Mohana Raju, K. J Colloid Interface Sci 2008, 318, 217.
19. Seok Lyoo, W.; Shik Ha, W. Polymer 1999, 40, 497.
20. Murali Mohan, Y.; Murthy, P. S. K.; Sreeramulu, J.; Mohana Raju, K. J Appl Polym Sci 2005, 98, 302.
21. Murali Mohan, Y.; Murthy, P. S. K.; Rao, K. M.; Sreeramulu, J.; Mohana Raju, K. J Appl Polym Sci 2005, 96, 1153.
22. Sambasivudu, K.; John, K.; Murthy, P. S. K.; Mani, Y.; Murali Mohan, Y.; Sreeramulu, J.; Mohana Raju, K. Int J Polym Mater 2007, 56, 1099.